

## Is Annual Recharge Coefficient a Valid Concept in Arid and Semi-Arid Region?

A manuscript submitted to *Hydrology and Earth System Sciences*

By

Yiben Cheng<sup>ab\*</sup>, Hongbin Zhan<sup>b\*</sup>, Wenbin Yang<sup>a\*</sup>, Hongzhong Dang<sup>a</sup>, Wei Li<sup>a</sup>

<sup>a</sup> Institute of Desertification Studies,

Chinese Academy of Forestry,

Haidian District, Beijing 100093, P. R. China ([chengyiben07@gmail.com](mailto:chengyiben07@gmail.com))

<sup>b</sup>Department of Geology & Geophysics,

Texas A&M University,

College Station, TX 77843-3115, USA. ([zhan@geos.tamu.edu](mailto:zhan@geos.tamu.edu))

\*Co-corresponding authors

March, 2017

**Abstract.** Deep soil recharge (DSR) (at depth more than 200 cm) is an important part of water circulation in arid and semi-arid regions. Quantitative monitoring of DSR is of great importance to assess water resources and to study water balance in arid and semi-arid regions. This study used a typical bare land on the Eastern margin of Mu Us Sandy Land in the Ordos basin of China as an example to illustrate a new lysimeter method of measuring DSR to examine if the annual recharge coefficient is valid or not in the study site, where the annual recharge efficient is the ratio of annual DSR over annual total precipitation. Positioning monitoring was done on precipitation and DSR measurements underneath mobile sand dunes from 2013 to 2015 in the study area. Results showed that use of an annual recharge coefficient for estimating DSR in bare sand land in arid and semi-arid regions is questionable and could lead to considerable errors. It appeared that DSR in those regions was influenced by precipitation pattern, and was closely correlated with spontaneous strong precipitation events (with precipitation greater than 10 mm) other than the total precipitation. This study showed that as much as 42% of precipitation in a single strong precipitation event can be transformed into DSR. During the observation period, the maximum annual DSR could make up to 24.33% of the annual precipitation. This study provided a reliable method of estimating DSR in sandy area of arid and semi-arid regions, which is valuable for managing groundwater resources and ecological restoration in those regions. It also provided strong evidence that the annual recharge coefficient was invalid for calculating DSR in arid and semi-arid regions. This study shows that DSR is closely related to the strong precipitation events, rather than to the average annual precipitation.

**Key words:** Deep soil recharge, deep soil infiltrometer, sandy land, new apparatus, rainfall, lysimeter

## Introduction

Recharge is an important source of groundwater budget and it is also a fundamental process that links the surface hydrological processes (e.g. precipitation), vadose zone process (e.g. infiltration and soil moisture dynamics), and the saturated zone process (e.g. groundwater flow) (Sanford, 2002; McWhorter and Sunada, 1977). How to accurately estimate recharge remains a persistent challenge and an active research topic in the hydrological science community over many decades (Gee and Hillel, 1988; Scanlon, 2013; Sanford, 2002). It is generally accepted that recharge is correlated to the precipitation in some fashions, and many studies adopt the concept of a recharge coefficient (Turkeltaub et al., 2015; Kalbus et al., 2006; Allocca et al., 2014), which is the ratio of the actual recharge to the precipitation, to estimate the recharge (Fiorillo et al., 2015; Allocca et al., 2014). The magnitude of such a recharge coefficient is controlled by a complex interplay of multiple factors such as moisture dynamics in the vadose zone (Schymanski et al., 2008), depth to the water table, vegetation, etc., and the recharge coefficient is often regarded as a temporally invariant value at a given location (Fiorillo et al., 2015; Min et al., 2017; Vauclin et al., 1979). Specifically, it is assumed to be primarily controlled by the total precipitation, not too much by the temporal fluctuation of precipitation events (Hickel and Zhang, 2006; Acworth et al., 2016). In this study, we will challenge the concept of using a constant recharge coefficient to estimate the recharge in arid and semi-arid regions based on a multi-year field investigation.

As water tables in many arid and semi-arid regions are relatively deep (greater than 2 meters below ground surface) (Williams, 1999; Soylu et al., 2011), recharge in those regions is named Deep Soil Recharge (DSR), which will be the concern of this study. DSR could ease the demand of sand-fixing vegetation on moisture during extremely dry seasons (Zhang et al.,

2001;Shou et al., 2016) , and it reduces water deficit, sustains life activities, and helps the vegetation to live through extreme droughts (Zhang et al., 2004). In this sense, DSR is an important factor of water cycle in arid and semi-arid regions (Adolph, 1947), and it could also provide much needed references for the stability analysis of sand-fixing vegetation (Li et al., 2004;Li et al., 2014). In the following, we will briefly review the existing methods of estimating DSR.

In general, there are three methods of measuring DSR in arid and semi-arid regions. The first is an empirical approach which assigns a constant recharge coefficient associated with a certain precipitation event (Allison et al., 1994;Jiménez-Martínez et al., 2010). The empirical approach is simple to use but it lacks a rigorous theoretical base, and the recharge coefficient has to be calibrated through a groundwater flow model in the region, which is often not available.

The second is a modeling approach involving numerical models such as HYDRUS (Šimůnek et al., 2012), SWAT (Arnold et al., 2012), UNSATH (Fayer, 2000), SWIM (Krysanova et al., 2005), SWAP (van Dam, 2000) to calculate DSR. Modeling is an efficiency way to test different hypothetical scenarios and it may be used to predict DSR in the future if the model is calibrated carefully. Detailed water balance models can be used for irrigated agriculture, but they usually cannot predict evapotranspiration accurately, especially when plants suffer seasonal water stress and plants cover is sparse (Gee and Hillel, 1988). When recharge is estimated as residual in water balance models, it can cause miscalculation as much as an order of magnitude (Scanlon, 2013;Voehler et al., 2014). When using soil water flow models with measured or estimated soil hydraulic conductivities and tension gradients, similar miscalculation can also occur (Nyman et al., 2014;Gee and Hillel, 1988). In addition, the modeling usually involves upscaling of parameter values over a spatially and temporally discretized mesh from

measurements which are made on specific moments and locations. Such an upscaling process is not always easy to execute and it could sometimes lead to serious errors. This is particularly true for arid and semi-arid regions where most precipitation may be episodic (occurring in short and unpredictable events) (Modarres and da Silva, 2007;Zhou et al., 2016), and may be confined to restricted portions of the area (Gee and Hillel, 1988).

The third includes a cluster of experimental techniques such as isotopic tracer (Klaus and McDonnell, 2013), water flux (Katz et al., 2016), and lysimeter (Scanlon, 2013). Among them, lysimeters are instruments that directly measure the hydrological cycle in infiltration, runoff and evaporation. Generally, this equipment is located in an open observation field or as a controlled device, working either solely or in groups (Good et al., 2015). In a typical lysimeter, soil are filled into a column surrounded by impermeable lateral boundaries thus water can only enter or leave the column from upper or lower boundaries (Duncan et al., 2016;Fritzsche et al., 2016). A drainage system is usually placed at the bottom (Glenn et al., 2013). The depth of soil in the column depends on the experimental purpose. Experiments can be done with the same type of soil at different depths in a single column, or in different columns but at the same depth. The soil surface can be cultivated with different crops or left alone as bare land. Observation can be recorded with weight or volume of water.

Application of above-mentioned methods for assessing DSR in arid and semi-arid regions has met a variety of challenges, primarily due to the fact that precipitation events often happen in the form of short pulses with highly variable intensity (Collins et al., 2014). The intermittent and unpredictable characteristics of precipitation events lead to highly variable moisture and nutrient levels in the soils (Beatley, 1974;Huxman et al., 2004). It is unclear how the precipitation

amount, time, and interval will affect the water moisture of arid and semi-arid regions, especially the change of deep soil water storage.

In this study, a new type of lysimeter is designed to accurately measure the amount of DSR in arid and semi-arid regions. With the help of a three-year (2013-2015) field investigation with this new lysimeter, one can answer the following question: Is the concept of an annual recharge coefficient valid or not for estimating DSR at a given location in an arid and semi-arid region? Before the introduction of this new type of lysimeter, it is necessary to briefly explain the challenges faced by the conventional lysimeter for studying DSR in arid and semi-arid regions.

## **2. Design of the new lysimeter for DSR measurement**

### **2.1. Problems with the conventional lysimeter methods in arid and semi-arid regions**

Lysimeters have been used to access the amount of water consumed by vegetation for more than three hundred years (Howell et al., 1991). The type of lysimeter that is specifically designed to measure evapotranspiration (ET), called precision weighing lysimeter, has been developed within the past six decades. In order to suit different requirements and needs, there are various designs of weighing lysimeters, with surface areas ranging from 1.0 m<sup>2</sup> to over 29 m<sup>2</sup> (Howell et al., 1991). The stored media mass and the type of scale such as diameter and height, are factors on which the accuracy of ET measurement depends, and many lysimeters have accuracies better than 0.05 mm (Howell et al., 1991). Figure 1A shows the schematic diagram of a conventional lysimeter installation in the field. It is basically a weight meter of soil with an open upper boundary at ground surface and a perforated bottom boundary and impermeable vertical side walls. The typical depth of lysimeters varies from 0.2 m to 2 m, but is rarely greater than 2.5 m (Howell et al., 1991). The horizontal cross-section area is usually in the range of 1 m<sup>2</sup> to 29 m<sup>2</sup>.

Precipitated water can freely infiltrate into the soil from the top and downward flow of water at the bottom of the lysimeter is collected (through the perforation) as a function of time to calculate the recharge. Alternatively, the weight of combined water and soil inside the lysimeter can be accurately measured using a weight gauge to reflect any soil moisture change. Such information, combined with infiltration or evaporation at the surface, can yield the information of downward water flux at the depth of lysimeter.

The following issues deserve special attention when applying the conventional lysimeter for measuring recharge. Firstly, soil layers are inevitably disturbed when installing the instrument, so the result may not reflect the actual recharge in native (undisturbed) soils (Weihermüller et al., 2007). Secondly, the cost is too high to use multiple lysimeters to observe large-scale infiltration (Stessel and Murphy, 1992). Thirdly, when precipitation strength is relatively light and concentrated, a large lysimeter cannot sensitively and rapidly measure DSR (Goldhamer et al., 1999; Farahani et al., 2007). The conventional lysimeter often cannot answer the following questions: To what soil layer can different levels of precipitations infiltrate? How much is the infiltration amount under different levels of precipitation? (Gee and Hillel, 1988; Ogle and Reynolds, 2004).

The conventional lysimeter as shown in Figure 1A may meet additional challenges when applied to arid and semi-arid regions. Firstly, the water table depths in arid and semi-arid regions may be much greater than the maximal depth of a conventional lysimeter (2.5 m). For instance, in Chagan Nur, southeast of Mu Us sandy land in the Ordos basin of China, the water table depth was found to be greater than 4 m. In the Gobi desert, the water table was reported to be at least 2.8 m deep (Ma et al., 2009). Therefore, the infiltration measured at the base of a conventional lysimeter may not represent the actual recharge that eventually enters the groundwater system.

157 Secondly, the measurement accuracy of lysimeter often declines for soils with deep plant roots  
158 because the depth of lysimeter installation is limited and it may be less than the depth of those  
159 roots at site, which by itself can be important pathways for water migration. Consequently, the  
160 measured recharge of such disturbed soil by lysimeter may not represent the in-situ recharge of  
161 the native (undisturbed) soil.

162 To resolve the above-mentioned issues faced by the conventional lysimeter, a new type of  
163 lysimeter is designed with specific considerations of the unique precipitation patterns and soil  
164 characteristics in arid and semi-arid regions. This new lysimeter is illustrated schematically in  
165 Figure 1(B).



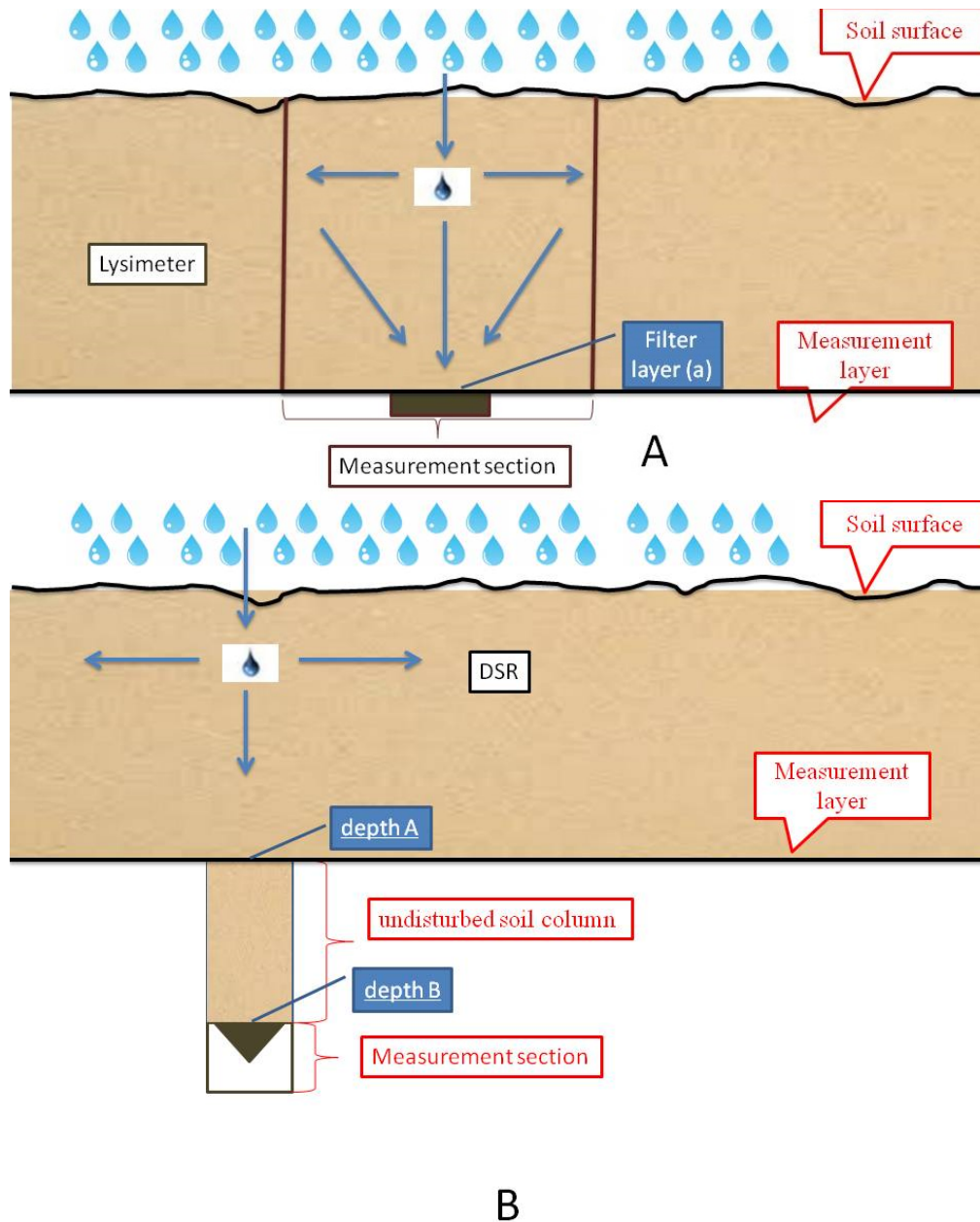


Figure 1. Schematic diagram of conventional lysimeter (A) and the new lysimeter (B).

## 2.2 Design of a new lysimeter for measuring DSR in arid and semi-arid regions

This new lysimeter has a few innovations (see Figure 1B) that can be outlined as follows. Instead of setting the upper boundary of the lysimeter at ground surface, the new design has its upper boundary at a designed depth (denoted as depth-A in Figure 1B) where infiltration will be

measured. A cylindrical container with a diameter of 20 cm to 40 cm with impermeable walls is installed from depth-A downward to a deeper depth-B. The length of AB is determined according to the capillary rise of the in-situ soil, which can be calculated using the average grain size of soils within AB. More specifically, the length of AB is greater than the capillary rise of soils within AB and it is usually great than 0.6 m (Liu et al., 2014). At the soil surface there is a device to measure the amount of the precipitation and at the base of the instrument (depth B), a water collection device is used to measure the amount of water exit the base.

Before the measurement, one necessary preparation is to inject water from the top of the instrument at depth-A using water pumps, the injection will stop until water starts to drip out from the base at depth-B. One usually has to wait 10 days to allow the water profile in column AB to become equilibrium. When water stops flowing out from depth-B, the soil water in the column is regarded as reaching its equilibrium state, in which the soil moisture at depth-B reaches the maximum field capacity. Under such an equilibrium status, the amount of infiltration entering the upper surface of the lysimeter will be discharged (with the same amount) from the base of the lysimeter after a certain delay time.

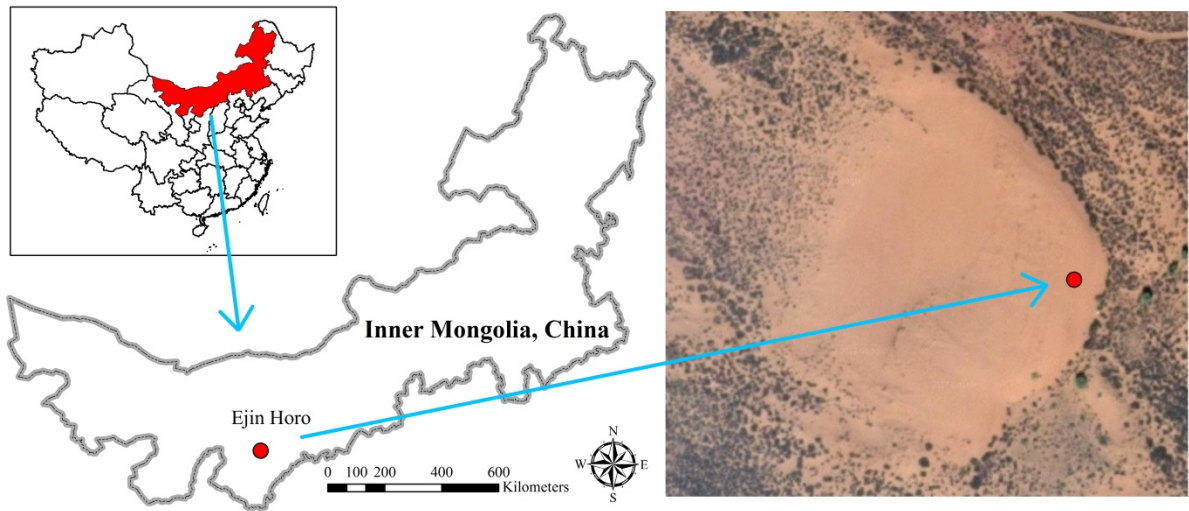
The proposed new method has a few innovative features that have not been considered in previous studies. Firstly, it can measure DSR at any given layer of a multi-layer soil system using a single apparatus installed in the field. Secondly, continuous real-time measurements can be recorded over any given time period, thus a time-series of DSR can be obtained, which will be very useful to understand the soil water dynamics at sandy area of arid and semi-arid regions. Thirdly, the apparatus is portable and easy to install, thus a large amount of data can be collected in various locations of a study area using multiple lysimeters, and spatial recharge distribution can also be obtained straightforwardly. This method is field tested in arid and semi-arid sandy

regions of western China. It provides key references for the evaluation of water resources, water balance, and the stability assessment of sand-fixing vegetation in arid and semi-arid areas. It also provides data that are much needed for evaluating soil water contents and groundwater resources of those areas. An important feature of this new lysimeter is that it can provide reliable DSR data to examine the concept of annual recharge coefficient when comparing with the precipitation data.

### **3. Field testing of the new apparatus**

#### **3.1 Description of the study area**

Figure 2 shows the location of the study which is located in Ejin Horo Banner, on the Eastern margin of Mu Us Sandy Land in the Ordos basin of China (geographic location: 39°05' N, 109°36' E; altitude: 1070-1556 m above mean sea level). The groundwater table between dunes are 5.3-6.8 m below ground surface. The climate is semi-arid continental monsoon climate zone. Precipitation concentrates from July to September, with relatively concentrated rainstorm. The average annual precipitation from 1960 to 2010 is 296.01 mm. The average annual temperature of this area is 6.5°C, with about 151 days of frost-free season, 1809 mm total evaporation, an average 2900 hours of sunshine, and an average wind speed of 3.24 m/s (Wu and Ci, 2002; Karnieli et al., 2014). The study area is located in relatively gentle mobile dunes, and the soil type is Aeolian sandy soil.



214



215

216

Figure 2. Geographic location of the experimental area.

217

218

219

220

221

In term of geological structure, Mu Us Sandy Land is in the Ordos basin, a large-scale syncline sedimentary basin with nearly north-south striking axis, and is of Mesozoic and Paleozoic ages. The basin covers an area of 640 km from north to south, and 400 km from east to west. The axis of syncline is off west, and the east and west wings are asymmetric. The east wing is Monoclinic of westward tilt with a width of more than 300 km. The west wing is made of

222 many fault-fold belts striking along the north-south direction and thrusting eastward with a width  
223 of less than 100 km. The southern boundary of the basin is Weibei plateau uplift. The southern  
224 part of this plateau uplift is descending in ladder-shape with blocks to Fenwei rift-subsidence  
225 basin. The northern boundary of this basin is Yimeng plateau uplift, with a lack of Lower  
226 Paleozoic, and its edge-fault is connected to Hetao fault basin. The basement of Ordos basin is of  
227 Precambrian crystalline metamorphic rocks.

228 Deposited in the basin are, in turn, Lower Paleozoic carbonate rocks, Upper Paleozoic-  
229 Mesozoic clastic rocks, and Cenozoic sedimentary rocks with a total depth of more than 6000 m.  
230 The discontinuous Cenozoic sediment is on top of the Mesozoic and Paleozoic layers, mainly of  
231 the Quaternary and partially of the Tertiary sediments. The Quaternary layer is mainly made of  
232 Aeolian sand and loess. Generally divided by a line along the Great Wall, the northwest land  
233 surface is mainly covered by wind-blown sand layers of varying thickness and a 40-120 m thick  
234 layer of alluvial-lacustrine; the southeast land surface is mainly covered by loess with various  
235 thickness from tens of meters to more than 200 m. Below the loess layers, there is Tertiary  
236 Pliocene mud rock with thickness of a few meters to tens of meters.

237 The hydro-stratigraphic units of the Ordos basin is quite complex, consisting of multiple  
238 connected aquifers. Following the order from bottom to top, the multiple aquifers are primarily  
239 made from various rock types of a karst aquifer consisting of Precambrian and Ordovician  
240 limestone, a fractured aquifer consisting of Carboniferous and Jurassic clastic rocks, a porous-  
241 fractured aquifer of Cretaceous clastic rocks, and a porous aquifer consisting of unconsolidated  
242 Cenozoic and Quaternary sediments. Generally speaking, Mu Us Sandy Land has relatively rich  
243 groundwater resources. The shallow groundwater reservoir is estimated to hold about 120.3  
244 billion metric tons of freshwater. Groundwater is mainly recharged by precipitation with an

annual average recharge amount of 1.4 billion metric tons. Fine sands are the dominating sediments observed in the experimental site. In the upper 200 cm soil layer in the experiment area, the percentage of fine sand (0.5-0.1 mm) are 88.56%, 77.88%, 88.23%, 88.89%, 90.28%, 83.90%, and 84.21% at depths of 0 cm, 10 cm, 30 cm, 60 cm, 90 cm, 150 cm, and 200 cm, respectively. The rest parts of the soil are primarily coarse sands. It is evident that the soil at the upper 200 cm is relatively homogeneous.

### **3.2 Statistical analysis of data**

Research on the relationship between precipitation and DSR of bare sand land in arid and semi-arid regions is beneficial to understand the soil-water dynamics of those regions. Because vegetation is absent, complexity related to transpiration process by plants is not a concern. Based on two time series of real-time data of precipitation and DSR, one can examine the relationship between DSR and precipitation. This study can serve as a basis for further study of DSR in semi-fixed and fixed sand lands with different fractional vegetation covers.

In September 1, 2012, mobile sand dune within the study site was set as the monitoring plot (geographic location: 39°05' N, 109°36' E; altitude: 1310 m) with the upper 220 cm soil profile excavated, and then backfilled using the excavated soil. Infiltration passing through the 200 cm depth is generally regarded as DSR in this study. It is worthwhile to point out that some other investigators may use a more or less different depth threshold for defining DSR. For instance, (Zhang et al., 2008) used 140 cm instead of 200 cm depth as the threshold to define DSR, It is found that the water table depth is greater than 4m in 2012-2015, so its influence to DSR is negligible. A precipitation sensor (AV-3665R, AVALON, United States; precision: 0.2 mm) was placed above ground at the site. Data acquirer (CR200X, Campbell, USA) was used to record DSR, of which DSR data were recorded every one hour, and the precipitation data were recorded

every half hour. In order to avoid the effect of freeze-and-thaw action, the experiment was conducted between April 1, 2013 and November 30, 2015. In this three years no runoff happen at the studied area.

The statistics of precipitation and DSR are shown in Table 1, which reveals that there is an obvious difference of precipitation at the experimental plot from 2013 to 2015. The annual precipitation is 83 mm in 2013, 205.6 mm in 2014, and 186.4 mm in 2015. This is to say, the annual precipitations in 2014 and 2015 are 2.48 and 2.25 times of that in 2013, respectively. Such a dramatic fluctuation and uneven distribution of annual precipitation is typical of arid and semi-arid regions. The corresponding annual DSR is 20.2 mm in 2013, 20.6 mm in 2014, and 9.2 mm in 2015. This is say that the annual DSR values in 2014 and 2015 are 1.02 and 0.46 of that in 2013. The annual DSR/precipitation ratios (or the so-called annual recharge coefficient) for 2013, 2014, and 2015 are 24.33%, 10%, and 4.94%, respectively.

It appears that there is no clear correlation between the annual DSR and the annual precipitation according to the data of 2013-2015. In another word, use of the annual recharge coefficient for the study site becomes questionable as such a coefficient implies that there is a close correlation between the annual DSR and the annual precipitation, which is not supported by the data of 2013-2015. Therefore, we will scrutinize the precipitation pattern and intensity more closely to decipher the connection of precipitation and DSR in the following.

Table 1: The annual precipitation-DSR relationship from 2013-2015.

Year	Precipitation	DSR	DSR/precipitation*100%
	(mm)	(mm)	

---

2013	83	20.2	24.33%
2014	205.6	20.6	10%
2015	186.4	9.2	4.94%

---

287

### 288 3.2.1 The relationship between precipitation pattern and DSR

289 Research on bare sandy soil water dynamic process usually focuses on temporal and vertical  
290 differences (Ritsema and Dekker, 1994;Postma et al., 1991). In term of temporal soil moisture  
291 variation over an annual cycle, the process could be divided as soil moisture replenishment,  
292 depletion, and relatively stable periods. In term of vertical soil moisture variation, soil water  
293 content usually first increases with depth and then decreases based on an interplay of mutual  
294 infiltration and evaporation processes. In general, soil could be divided as a surface dry sand  
295 layer, a layer with drastic moisture change, and a layer with relatively stable moisture content.  
296 Specifically, the soil deeper than 160 cm in arid and semi-arid regions would have a relatively  
297 stable moisture content. This is because of two reasons. Firstly, soil water will not be up-taken to  
298 the surface by capillary force at such depths; secondly, ground water table in arid and semi-arid  
299 regions is usually much lower than 160 cm.

300 In our study site, 2013 is an especially dry year with only 83 mm precipitation compared to  
301 296.01 mm of average annual rainfall calculated over a period from 1960 to 2010. The  
302 precipitation and DSR patterns of 2013 are shown in Figure 3. The measurement accuracy of the  
303 lysimeter is 0.2 mm. During the observation period from April 1 to November 30, there are  
304 totally 25 recorded precipitation events, mostly concentrated in the period from May to August.



305 There is a one-time strongest precipitation event with a 24-hour precipitation amount reaching 32  
306 mm in August 3. The DSR correlated to this event can be identified from September 21 to  
307 November 30 and reaches 17.2 mm. The delay time from precipitation event to the start of DSR  
308 is approximately 48 days. The DSR/precipitation ratio for this particular event is as high as  
309 53.75%. Such a DSR/precipitation ratio appears to be the highest in 2013. It is worth to note that  
310 although the strongest precipitation event at August 3 contributes the greatest to DSR observed  
311 from September 21 to November 30, a few precipitation events with amount of 6.6 mm prior to  
312 this strongest precipitation event also contribute a minor part for DSR from July 27 to August 1.  
313 It is also notable that the DSR/precipitation ratio for the strongest precipitation event is  
314 substantially higher than the average annual recharge coefficient of 24.33% in 2013. This leads  
315 to the conclusion that DSR is closely related to the strong precipitation events, rather than to the  
316 average annual precipitation.

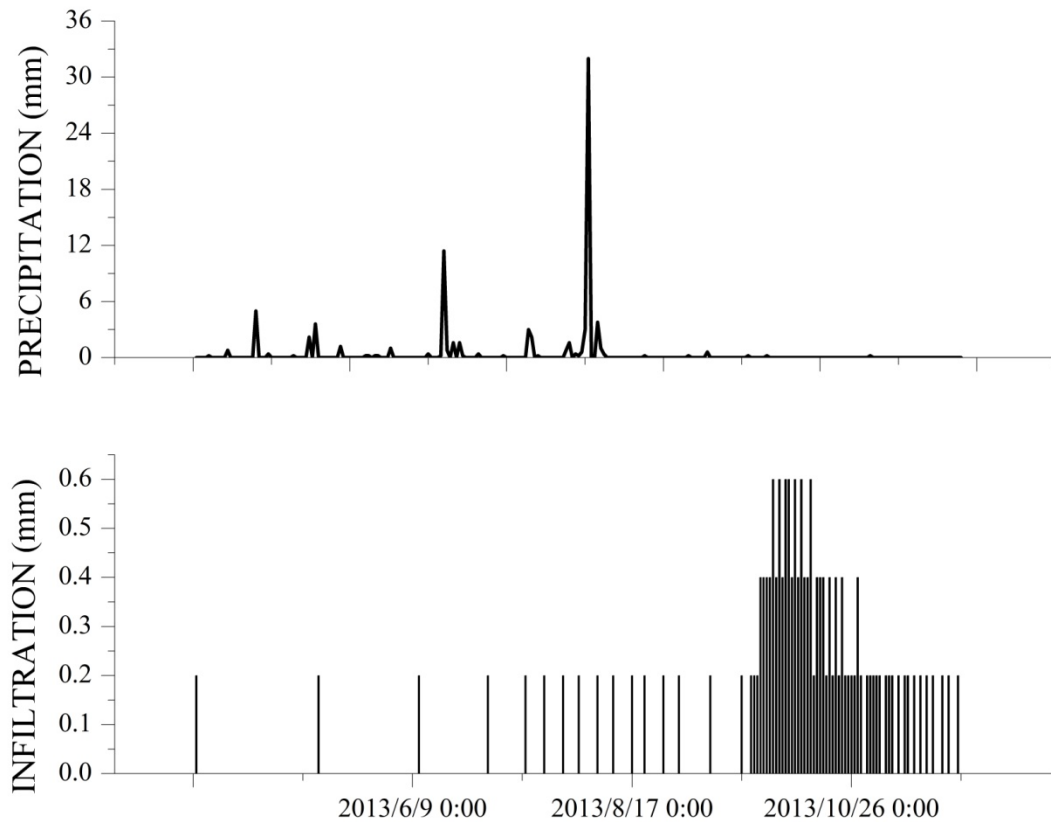


Figure 3: Precipitation and DSR patterns in 2013.

In 2014, the annual precipitation is 205.6 mm, and DSR is 20.6 mm, leading to a 10% annual average recharge coefficient, which is less than half of that in 2013. As shown in Figure 4, the frequency of precipitation events in 2014 is obviously higher than that of 2013. From April 1 to November 30, there are total 68 times of precipitation events, compared to 41 times in 2013. Furthermore, the precipitation distribution in 2014 is more uniform than that in 2013. Specifically, precipitation events are concentrated in the period from June to August, with the highest 24-hour accumulative precipitation of 15 mm on July 30. As shown in Figure 4, recorded DSR data cover a period from April 1 to November 30, and the maximum DSR occurs in October 1. Because the experimental plot is located in a transition zone between arid and semi-arid regions, summer evaporation is strong, leading to relatively less DSR during the summer

329 season. While during the period from September 1 to November 30, atmospheric temperature  
330 drops and sunshine duration becomes shorter, which results in less surface evaporation and  
331 greater DSR during this period. Compares to 2013, there are more summer precipitation events  
332 in 2014. That is one reason why precipitation in 2014 (205.6 mm) is greater than 2013 (83 mm)  
333 but the overall DSR in 2014 is less than that in 2013.

334 The strongest single-day precipitation in 2014 is 15 mm (occurred in July 30), which is less than  
335 half of the strongest single-day precipitation event of 32 mm occurred in 2013 (August 3), annual  
336 DSR/precipitation ratio of 2013 is 24.33% but in 2014 is 10%. This once again supports the  
337 conclusion that the strong precipitation events rather than the average annual precipitation are  
338 mostly responsible for the average annual DSR. This is the other reason why precipitation in  
339 2014 (205.6 mm) is greater than 2013 (83 mm) but the overall DSR in 2014 is less than that in  
340 2013.

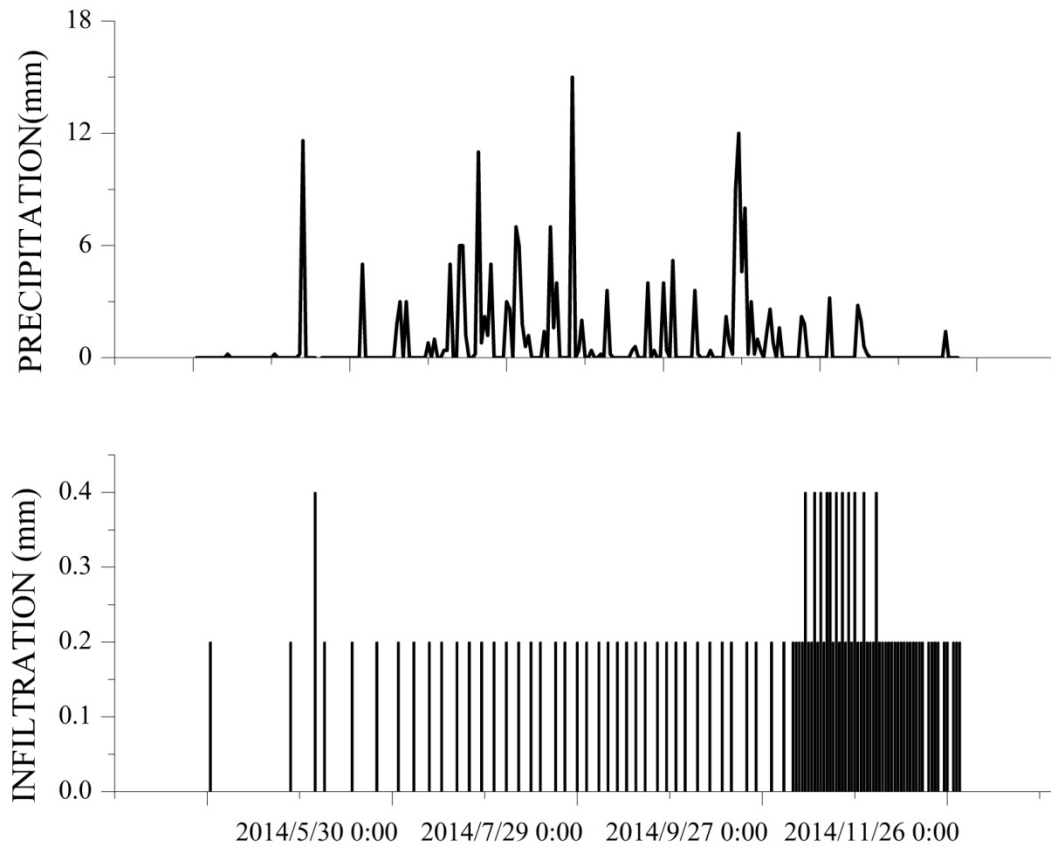


Figure 4: Precipitation and DSR patterns in 2014.

As shown in Figure 5, the total annual precipitation of 2015 is 186.4 mm, and DSR is 9.2 mm, leading to a 4.94% annual average recharge coefficient, which is significantly smaller than of 2013 (24.33%) and 2014 (10%). There are total 66 observable precipitation events in 2015. Such precipitation events are mostly concentrated from April 4 to July 6, with a total precipitation of 155 mm during this period, which represents 83.15% of the total precipitation in 2015. The measured DSR from April 4 to July 6 is only 7 mm, representing 77.78% of the total DSR in 2015. Throughout 2015, two strongest precipitation events happens on April 4 and June 5, both 24-hour precipitation events reach 17.2 mm. We observe a single-day DSR peak of 0.8 mm 36 days after April 4, one of the two greatest single-day DSR values observed in 2015, but

no peak value of DSR response to the strong precipitation in June 5. As explained before, summer stronger evaporation leads to relatively less DSR during the summer season compared with other seasons. The third greatest precipitation is 16.8 mm in October 5, which leads to a peak value of 0.8 mm of DSR in October 21, with a 16-day delay time. If comparing the precipitation events occurred in April 4 (17.2 mm) and October 5 (16.8 mm), one can see that these two precipitation events are similar in strength (17.2 mm for April 4 and 16.8 mm for October 5) but different in the DSR delay time (36 days for April 4 and 16 days for October 5). Comparing two precipitation events which are similar in strength but different in the DSR delay time, temperature is the most likely factor for such a delay time, so this lead to a conclusion that temperature influences the DSR rate. To investigate how the soil temperature affects the DSR rate, further field experiments are needed in the future study.

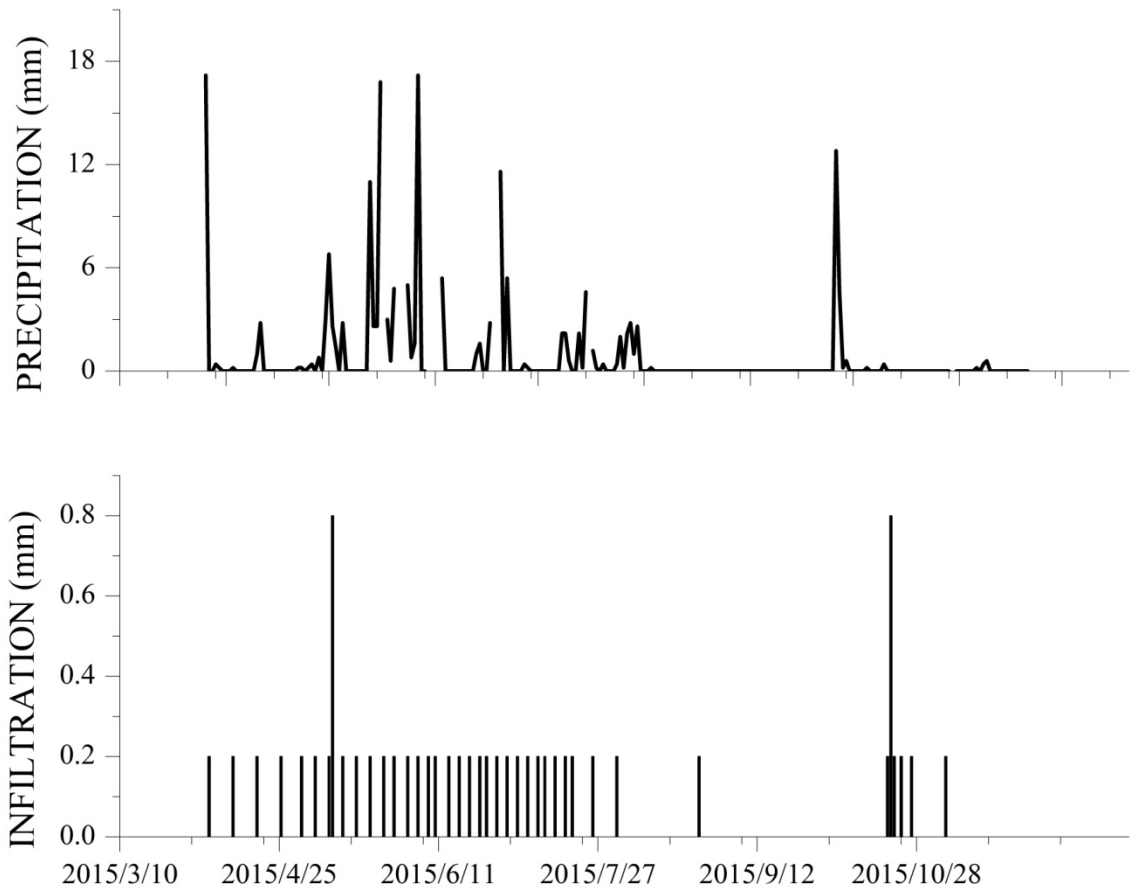


Figure 5: Precipitation and DSR patterns in 2015.

### 3.2.2 Relationship between precipitation intensity and DSR

Based on observational data and analysis in 3.2.1, one can see that precipitation intensity, to some extent, influences DSR. For the sake of illustration, the precipitation intensity for bare sand land is roughly classified into light, moderate, and strong events with precipitation amount less than 6 mm, between 6 mm to 10 mm, and greater than 10 mm, respectively. In general, light precipitation rarely can reach the soil zone deeper than 40 cm because of evaporation, thus it makes almost no contribution to DSR (Zhang et al., 2016). Such a classification may be revised under different vegetation covering conditions in different regions (Kosmas et al., 2000).

According to this classification, statistics of moderate to strong precipitation events and their percentage shares in the annual precipitation from 2013 to 2015 are shown in Table 2. In 2013, there are only two precipitation events with intensity greater than 6 mm. The total amount of these two precipitation events is 43.4 mm, which represents 52.29% of the annual precipitation in 2013. In 2014, there are 11 precipitation events with intensity greater than 6 mm, much more frequent than that of 2013 (2 times) and moderately more frequent than that of 2015 (8 times). The total moderate to strong precipitation in 2014 is 98.6 mm, representing 47.96% of the annual precipitation in 2014. In 2015, there are 8 precipitation events with intensity greater than 6 mm, accounting for 53.54% of the annual precipitation in 2015.

Among these three years, 2015 has the largest percentage of moderate to strong precipitation over the annual precipitation. However, at this same year, one has seen the smallest ratio of annual DSR/precipitation ratio or annual recharge coefficient (see Table 1). This implies that the annual DSR does not seem to be positively correlated to the annual total precipitation. This finding has a few profound consequences. It basically states that assigning a constant annual

recharge coefficient for a particular soil regardless of precipitation patterns is not a good practice, because annual DSR is not always proportional to the total annual precipitation. Instead, it appears to be more closely related to individual precipitation events stronger than 10 mm.

Table 2: Percentage of valid precipitation in total precipitation amount.

Year	Number of precipitation >6mm (24 hr cumulative)	Amount of precipitation >6mm (mm)	Valid precipitation /annual precipitation (%)
2013	2	43.4	52.29
2014	11	98.6	47.96
2015	8	99.8	53.54

Table 3 lists the number of strong precipitation (with amount greater than 10 mm) and also the strongest precipitation amount for each of 2013, 2014 and 2015. In 2013, there are only 2 strong precipitation events, but the maximum single-day precipitation amount reaches 32 mm (August 3). The accumulative strong precipitation of 2013 is 43.4 mm, which is 52.28% of the annual precipitation in 2013. In 2014, there are 4 strong precipitation events and the maximum single-day precipitation amount is 15 mm. The accumulative strong precipitation of 2014 is 49.6 mm, which is 24.12% of the annual precipitation in 2014. In 2015, there are 6 strong precipitation events, and the maximum single-day precipitation amount is 17.2 mm. The accumulative strong precipitation of 2015 is 86.6 mm, which represents 46.46% of the annual

precipitation in 2015. The annual DSR versus annual precipitation ratios are 24.33%, 10%, and 4.94% for 2013, 2014, and 2015, respectively.

As shown in Table 3, the strongest single-day precipitation (32 mm in 2013) appears to affect DSR the most in 2013. For 2014 and 2015, as the strongest precipitation events in these two years are significantly smaller than that in 2013. Such a positive correlation is particularly strong for 2013 which has the largest maximum precipitation event of 32mm, show that strong single-day precipitation affects DSR. This positive correlation is weaker for 2014 and 2015 which have moderate and somewhat similar maximum precipitation events (15mm and 17.2mm, respectively). But for 2014 and 2015, as shown in Figure 4 and Figure 5, precipitation pattern affect more for in 2014 precipitation is more average distribution from April to November but in 2015 precipitation is Concentrated from May to June.

In summary, one may conclude that annual DSR in arid and semi-arid regions mainly rely on strong precipitation events, but the determination of the threshold for strong precipitation events that directly contribute to DSR is still unclear and requires further investigation.

Table 3: Inter-annual statistics of strong precipitation and its percentage in total annual precipitation amount.

Year	Number of strong precipitation	Maximum precipitation event(mm)	Annual DSR (mm)	Annual DSR /annual precipitation (%)
2013	2	32	20.2	24.33
2014	4	15	20.6	10



2015	6	17.2	9.2	4.94
------	---	------	-----	------

417

418

419

420

421

422

423

424

425

426

427

Under the condition of continuous precipitation, it may be difficult to discretize precipitation into individual events. The following example illustrates a procedure to deal with this situation. As shown in Figure 6, there is a 13-days continuous precipitation process in 2013 from July 27 to August 8, and the accumulative precipitation is 43.8 mm. The start of a continuous DSR distribution corresponding to this 13-day continuous precipitation event is observed 3 days after the end of this precipitation process, and the peak value of DSR occurs 46 days after the end of this precipitation process. The DSR distribution gradually recedes to zero around 78 days after the end of the precipitation process. The accumulative DSR amount over a 75-day period is 18.4 mm. The ratio of the 75-day cumulative DSR over the 13-day precipitation event is 42%.

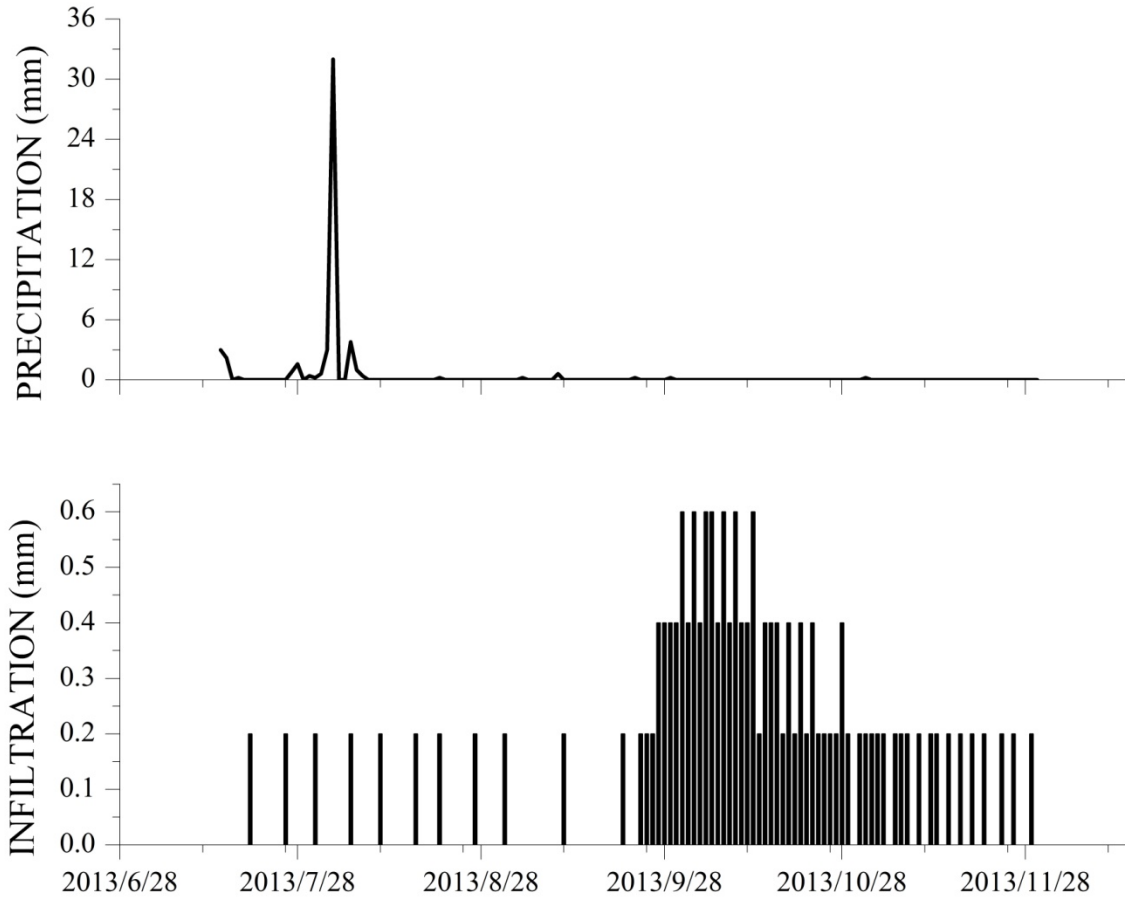


Figure 6: One-day intensive precipitation's contribution to DSR in 2013.

#### 4. Discussion

This improved lysimeter is on the real-time dynamic monitoring of DSR, and it provides reliable evidence for an accurate evaluation of precipitation-related recharging capability of bare sand lands in arid and semi-arid regions. However, there are a number of issues that deserves further attention and requires additional investigations in the future. The moisture evaporation, the soil absorption of moisture, and the water infiltration of post-evaporative redistribution, are all very complex processes, especially in arid and semi-arid regions. It is sometimes difficult to clearly distinguish the amount of evaporation and DSR with conventional methods as outlined in the introduction. This study selects precipitation and infiltration data during the period from April 1 to November 30, so the influence of freeze-thaw process during winter is avoided, and

the experimental design and data analysis is simplified. For this reasons, the next steps should be a full-term monitoring, a systematic study on DSR, as well as a study on the soil temperature and daily temperature influences on DSR.

Although this experiment does not address the issue of soil temperature effect on DSR in great details, the relationship between DSR and soil temperature is evident. In general, a higher temperature means a stronger evaporation demand, thus an often smaller DSR.

Through the analysis of this study, one can see that the use of an annual recharge coefficient for the study area is not supported by the data collected from the new lysimeter, as the annual recharge is not positively correlated with the annual total precipitation. Instead, we find that the recharge is somewhat positively correlated with a few strong precipitation events (greater than 10 mm), and very closely correlated with the strongest precipitation event (considerably greater than 10 mm). It is probably reasonable to assign different weighting factors for different precipitation strengths to calculate DSR. However, the threshold to define a strong precipitation event that makes direct contribution to DSR is not precisely quantified, and this is a subject that should be investigated in more details in the future. The determination of weighting factors for different precipitation strengths is also a subject requires further investigation.

## **5. Conclusions**

This study uses a newly designed lysimeter to study three consecutive years (2013-2015) of DSR underneath bare sand land on the Eastern margin of Mu Us Sandy Land in the Ordos basin of China. The objective is to identify the characteristics of the DSR distribution and the factors affecting the DSR distribution. Specifically, we like to examine if the commonly used recharge coefficient concept can be applied for arid and semi-arid regions such as the Eastern margin of

Mu Us Sandy Land of China.

The following conclusions can be drawn from this study:

- (1) The annual recharge coefficient concept is generally inapplicable for estimating DSR in the study site.
- (2) Precipitation pattern including precipitation intensity and precipitation season significantly influences DSR.
- (3) The temperature influences the DSR/precipitation ratio, which is less in summer as in other seasons, given the similar precipitation intensity.
- (4) DSR is not correlated with the annual precipitation. Instead, it is correlated with the strong precipitation (greater than 10 mm) events at the site. However, quantitative determination of the thresholds for such strong precipitation events that makes direct contribution to DSR is not entirely understood. Further investigation is needed on this subject.

**Acknowledgements.** This study was supported with research grants from the Ministry of Science and Technology of the People's Republic of China (2013CB429901).

## References

- Acworth, R. I., Rau, G. C., Cuthbert, M. O., Jensen, E., and Leggett, K.: Long-term spatio-temporal precipitation variability in arid-zone Australia and implications for groundwater recharge, *Hydrogeology Journal*, 24, 905-921, 2016.
- Adolph, E. F.: *Physiology of Man in the Desert*, Physiology of Man in the Desert., 1947.
- Allison, G., Gee, G., and Tyler, S.: Vadose-zone techniques for estimating groundwater recharge in arid and semiarid regions, *Soil Science Society of America Journal*, 58, 6-14, 1994.
- Allocca, V., Manna, F., and De Vita, P.: Estimating annual groundwater recharge coefficient for karst aquifers of the southern Apennines (Italy), *Hydrology and Earth System Sciences*, 18, 803, 2014.
- Arnold, J. G., Moriasi, D. N., Gassman, P. W., Abbaspour, K. C., White, M. J., Srinivasan, R., Santhi, C., Harmel, R., Van Griensven, A., and Van Liew, M. W.: SWAT: Model use, calibration, and validation, *Transactions of the ASABE*, 55, 1491-1508, 2012.
- Beatley, J. C.: Phenological events and their environmental triggers in Mojave Desert ecosystems, *Ecology*, 55, 856-863, 1974.

494 Collins, S. L., Belnap, J., Grimm, N., Rudgers, J., Dahm, C. N., D'odorico, P., Litvak, M., Natvig, D., Peters, D.  
 495 C., and Pockman, W.: A multiscale, hierarchical model of pulse dynamics in arid-land ecosystems, *Annual*  
 496 *Review of Ecology, Evolution, and Systematics*, 45, 397-419, 2014.  
 497 Duncan, M., Srinivasan, M., and McMillan, H.: Field measurement of groundwater recharge under  
 498 irrigation in Canterbury, New Zealand, using drainage lysimeters, *Agricultural Water Management*, 166,  
 499 17-32, 2016.  
 500 Farahani, H., Howell, T., Shuttleworth, W., and Bausch, W.: Evapotranspiration: progress in  
 501 measurement and modeling in agriculture, *Trans. Asabe*, 50, 1627-1638, 2007.  
 502 Fayer, M. J.: UNSAT-H version 3.0: Unsaturated soil water and heat flow model. Theory, user manual,  
 503 and examples, Pacific Northwest National Laboratory, 13249, 2000.  
 504 Fiorillo, F., Pagnozzi, M., and Ventafridda, G.: A model to simulate recharge processes of karst massifs,  
 505 *Hydrological Processes*, 29, 2301-2314, 2015.  
 506 Fritzsche, A., Pagels, B., and Totsche, K. U.: The composition of mobile matter in a floodplain topsoil: A  
 507 comparative study with soil columns and field lysimeters, *Journal of Plant Nutrition and Soil Science*, 179,  
 508 18-28, 2016.  
 509 Gee, G. W., and Hillel, D.: Groundwater recharge in arid regions: review and critique of estimation  
 510 methods, *Hydrological Processes*, 2, 255-266, 1988.  
 511 Glenn, E. P., Anday, T., Chaturvedi, R., Martinez-Garcia, R., Pearlstein, S., Soliz, D., Nelson, S. G., and  
 512 Felger, R. S.: Three halophytes for saline-water agriculture: An oilseed, a forage and a grain crop,  
 513 *Environmental and Experimental Botany*, 92, 110-121, 2013.  
 514 Goldhamer, D. A., Fereres, E., Mata, M., Girona, J., and Cohen, M.: Sensitivity of continuous and discrete  
 515 plant and soil water status monitoring in peach trees subjected to deficit irrigation, *Journal of the*  
 516 *American Society for Horticultural Science*, 124, 437-444, 1999.  
 517 Good, S. P., Noone, D., and Bowen, G.: Hydrologic connectivity constrains partitioning of global  
 518 terrestrial water fluxes, *Science*, 349, 175-177, 2015.  
 519 Hickel, K., and Zhang, L.: Estimating the impact of rainfall seasonality on mean annual water balance  
 520 using a top-down approach, *Journal of Hydrology*, 331, 409-424, 2006.  
 521 Howell, T. A., Schneider, A. D., and Jensen, M. E.: History of lysimeter design and use for  
 522 evapotranspiration measurements, *Lysimeters for Evapotranspiration and Environmental*  
 523 *Measurements*, 1991, 1-9,  
 524 Huxman, T. E., Snyder, K. A., Tissue, D., Leffler, A. J., Ogle, K., Pockman, W. T., Sandquist, D. R., Potts, D.  
 525 L., and Schwinning, S.: Precipitation pulses and carbon fluxes in semiarid and arid ecosystems, *Oecologia*,  
 526 141, 254-268, 2004.  
 527 Jiménez-Martínez, J., Candela, L., Molinero, J., and Tamoh, K.: Groundwater recharge in irrigated semi-  
 528 arid areas: quantitative hydrological modelling and sensitivity analysis, *Hydrogeology Journal*, 18, 1811-  
 529 1824, 2010.  
 530 Kalbus, E., Reinstorf, F., and Schirmer, M.: Measuring methods for groundwater? surface water  
 531 interactions: a review, *Hydrology and Earth System Sciences Discussions*, 10, 873-887, 2006.  
 532 Karnieli, A., Qin, Z., Wu, B., Panov, N., and Yan, F.: Spatio-temporal dynamics of land-use and land-cover  
 533 in the Mu Us sandy land, China, using the change vector analysis technique, *Remote Sensing*, 6, 9316-  
 534 9339, 2014.  
 535 Katz, B. S., Stotler, R. L., Hirmas, D., Ludvigson, G., Smith, J. J., and Whittemore, D. O.: Geochemical  
 536 Recharge Estimation and the Effects of a Declining Water Table, *Vadose Zone Journal*, 15, 2016.  
 537 Klaus, J., and McDonnell, J.: Hydrograph separation using stable isotopes: review and evaluation, *Journal*  
 538 *of Hydrology*, 505, 47-64, 2013.  
 539 Kosmas, C., Danalatos, N., and Gerontidis, S.: The effect of land parameters on vegetation performance  
 540 and degree of erosion under Mediterranean conditions, *Catena*, 40, 3-17, 2000.

541 Krysanova, V., Hattermann, F., and Wechsung, F.: Development of the ecohydrological model SWIM for  
 542 regional impact studies and vulnerability assessment, *Hydrological Processes*, 19, 763-783, 2005.  
 543 Li, X., Zhang, Z., Tan, H., Gao, Y., Liu, L., and Wang, X.: Ecological restoration and recovery in the wind-  
 544 blown sand hazard areas of northern China: relationship between soil water and carrying capacity for  
 545 vegetation in the Tengger Desert, *Science China. Life Sciences*, 57, 539, 2014.  
 546 Li, X. R., Ma, F. Y., Xiao, H. L., Wang, X. P., and Kim, K. C.: Long-term effects of revegetation on soil water  
 547 content of sand dunes in arid region of Northern China, *Journal of Arid Environments*, 57, 1-16, 2004.  
 548 Liu, Q., Yasufuku, N., Miao, J., and Ren, J.: An approach for quick estimation of maximum height of  
 549 capillary rise, *Soils and Foundations*, 54, 1241-1245, 2014.  
 550 Ma, J., Ding, Z., Edmunds, W. M., Gates, J. B., and Huang, T.: Limits to recharge of groundwater from  
 551 Tibetan plateau to the Gobi desert, implications for water management in the mountain front, *Journal of*  
 552 *Hydrology*, 364, 128-141, 2009.  
 553 McWhorter, D. B., and Sunada, D. K.: Ground-water hydrology and hydraulics, Water Resources  
 554 Publication, 1977.  
 555 Min, L., Shen, Y., Pei, H., and Jing, B.: Characterizing deep vadose zone water movement and solute  
 556 transport under typical irrigated cropland in the North China Plain, *Hydrological Processes*, 2017.  
 557 Modarres, R., and da Silva, V. d. P. R.: Rainfall trends in arid and semi-arid regions of Iran, *Journal of Arid*  
 558 *Environments*, 70, 344-355, 2007.  
 559 Nyman, P., Sheridan, G. J., Smith, H. G., and Lane, P. N.: Modeling the effects of surface storage,  
 560 macropore flow and water repellency on infiltration after wildfire, *Journal of Hydrology*, 513, 301-313,  
 561 2014.  
 562 Ogle, K., and Reynolds, J. F.: Plant responses to precipitation in desert ecosystems: integrating functional  
 563 types, pulses, thresholds, and delays, *Oecologia*, 141, 282-294, 2004.  
 564 Postma, D., Boesen, C., Kristiansen, H., and Larsen, F.: Nitrate reduction in an unconfined sandy aquifer:  
 565 water chemistry, reduction processes, and geochemical modeling, *Water Resources Research*, 27, 2027-  
 566 2045, 1991.  
 567 Ritsema, C. J., and Dekker, L. W.: How water moves in a water repellent sandy soil: 2. Dynamics of  
 568 fingered flow, *Water Resources Research*, 30, 2519-2531, 1994.  
 569 Sanford, W.: Recharge and groundwater models: an overview, *Hydrogeology Journal*, 10, 110-120, 2002.  
 570 Scanlon, B. R.: Evaluation of methods of estimating recharge in semiarid and arid regions in the  
 571 southwestern US, *Groundwater recharge in a desert environment: The southwestern United States*, 235-  
 572 254, 2013.  
 573 Schymanski, S. J., Sivapalan, M., Roderick, M., Beringer, J., and Hutley, L.: An optimality-based model of  
 574 the coupled soil moisture and root dynamics, *Hydrology and Earth System Sciences Discussions*, 12, 913-  
 575 932, 2008.  
 576 Shou, W., Musa, A., Liu, Z., Qian, J., Niu, C., and Guo, Y.: Rainfall partitioning characteristics of three  
 577 typical sand-fixing shrubs in Horqin Sand Land, north-eastern China, *Hydrology Research*, nh2016177,  
 578 2016.  
 579 Šimůnek, J., Van Genuchten, M. T., and Šejna, M.: HYDRUS: Model use, calibration, and validation, *Trans.*  
 580 *Asabe*, 55, 1261-1274, 2012.  
 581 Soylu, M., Istanbuluoglu, E., Lenters, J., and Wang, T.: Quantifying the impact of groundwater depth on  
 582 evapotranspiration in a semi-arid grassland region, *Hydrology and Earth System Sciences*, 15, 787-806,  
 583 2011.  
 584 Stessel, R., and Murphy, R.: A lysimeter study of the aerobic landfill concept, *Waste Management &*  
 585 *Research*, 10, 485-503, 1992.  
 586 Turkeltaub, T., Kurtzman, D., Bel, G., and Dahan, O.: Examination of groundwater recharge with a  
 587 calibrated/validated flow model of the deep vadose zone, *Journal of Hydrology*, 522, 618-627, 2015.

588 van Dam, J. C.: Field-scale water flow and solute transport: SWAP model concepts, parameter estimation  
589 and case studies, [sn], 2000.

590 Vauclin, M., Khanji, D., and Vachaud, G.: Experimental and numerical study of a transient,  
591 two-dimensional unsaturated-saturated water table recharge problem, *Water Resources Research*, 15,  
592 1089-1101, 1979.

593 Voeckler, H. M., Allen, D. M., and Alila, Y.: Modeling coupled surface water–Groundwater processes in a  
594 small mountainous headwater catchment, *Journal of Hydrology*, 517, 1089-1106, 2014.

595 Weihermüller, L., Siemens, J., Deurer, M., Knoblauch, S., Rupp, H., Göttlein, A., and Pütz, T.: In situ soil  
596 water extraction: a review, *Journal of environmental quality*, 36, 1735-1748, 2007.

597 Williams, W. D.: Salinisation: A major threat to water resources in the arid and semi-arid regions of the  
598 world, *Lakes & Reservoirs: Research & Management*, 4, 85-91, 1999.

599 Wu, B., and Ci, L. J.: Landscape change and desertification development in the Mu Us Sandland,  
600 Northern China, *Journal of Arid Environments*, 50, 429-444, 2002.

601 Zhang, J., Felzer, B. S., and Troy, T. J.: Extreme precipitation drives groundwater recharge: the Northern  
602 High Plains Aquifer, central United States, 2016.

603 Zhang, L., Dawes, W., and Walker, G.: Response of mean annual evapotranspiration to vegetation  
604 changes at catchment scale, *Water resources research*, 37, 701-708, 2001.

605 Zhang, Y., Kendy, E., Qiang, Y., Changming, L., Yanjun, S., and Hongyong, S.: Effect of soil water deficit on  
606 evapotranspiration, crop yield, and water use efficiency in the North China Plain, *Agricultural Water  
607 Management*, 64, 107-122, 2004.

608 Zhang, Z.-S., Liu, L.-C., Li, X.-R., Zhang, J.-G., He, M.-Z., and Tan, H.-J.: Evaporation properties of a  
609 revegetated area of the Tengger Desert, North China, *Journal of arid Environments*, 72, 964-973, 2008.

610 Zhou, J., Fu, B., Gao, G., Lü, Y., Liu, Y., Lü, N., and Wang, S.: Effects of precipitation and restoration  
611 vegetation on soil erosion in a semi-arid environment in the Loess Plateau, China, *Catena*, 137, 1-11,  
612 2016.

613